

The Chicken Egg Genotoxicity Assay (CEGA): Assessing Target Tissue Exposure and Metabolism in the Embryo-Fetal Chicken Livers

Yax Thakkar¹, Tetyana Kobets², Anne Marie Api¹, Jian-Dong Duan³, and Gary Williams²

¹RIFM

²New York Medical College

³Deceased, Former address: New York Medical College

January 29, 2025

Abstract

The Chicken Egg Genotoxicity Assay (CEGA) is an avian egg-based model that utilizes the livers of developing chicken embryo-fetuses to assess the ability of chemicals to produce direct DNA damage. The main goal of the study was to evaluate target tissue exposure and metabolism in the CEGA to assess its suitability as a biologically relevant new approach methodology (NAM) for detecting genotoxic potential of chemicals. An imaging study using two-photon excitation microscopy following administration of a fluorescent dye (acridine orange) verified that chemicals following administration into the air sac of the fertilized chicken egg reach the target organ, liver. Additionally, a metabolism study using liquid chromatography with high resolution mass spectrometry (LC/MS), conducted after administration of benzo[a]pyrene (B(a)P) according to the CEGA protocol, confirmed the formation of sufficient amounts of reactive metabolite(s) responsible for genotoxic effects of a parent compound upon reaching the target tissue. Moreover, RNA sequencing study revealed that B(a)P in embryo-fetal chicken livers significantly upregulated several genes responsible for the activity of CYP1A1 enzyme which is critical for bioactivation of B(a)P. These findings support previous reports in CEGA, where B(a)P produced DNA damage in the liver tissues in the form of strand breaks and adducts. Overall, the findings in the study support the conclusion that the CEGA can be considered a robust potential alternative to animal testing strategy for assessing the genotoxic potential of chemicals

INTRODUCTION

Carcinogenic chemicals can be broadly classified based on their mode of action, with a major focus on genotoxic and non-genotoxic mechanisms. Genotoxic carcinogens directly interact with the genetic material of cells, causing mutations, chromosomal fragmentation, or rearrangements. These alterations can disrupt normal cellular functions, leading to uncontrolled cell proliferation and ultimately cancer. Genotoxicity of chemicals can be evaluated in various *in vitro* and *in vivo* assays, which are mainly designed to evaluate mutagenicity potential, chromosomal damage, and DNA damage /repair pathways interruption. Due to the recent restrictions in the use of *in vivo* genotoxicity assays, there is a need for biologically relevant new approach methodologies (NAMs) to be used as animal alternatives for evaluating genotoxic potential of chemicals that had *in vitro* positive results. The Chicken and related Turkey Egg Genotoxicity Assays (CEGA and TEGA, respectively) (Williams et al., 2014; Iatropoulos et al., 2017; Kobets et al., 2018b; Kobets et al., 2016; 2018a), were developed as metabolically competent (Kobets et al., 2018b; Perrone et al., 2004) NAMs for genotoxicity screening to potentially replace short-term *in vivo* studies required for human safety assessment. CEGA uses fertilized, specific pathogen free eggs from the white leghorn chicken of

undetermined sex. Since the termination of the embryos in CEGA is conducted on incubation day 11, at least 10 days before hatching, discomfort to the organism is precluded, as the nervous system of the embryos is not completely developed (Hughes 1953). Thus, in compliance with Animals (Scientific Procedures) Act 1986, CEGA is not considered to be an animal model. CEGA evaluates two different endpoints, DNA adducts by the means of the NPL assay (Phillips and Arlt, 2014; Randerath et al., 1981; Reddy and Randerath, 1986) and DNA strand breaks using the alkaline single cell gel electrophoresis (comet) assay (Brendler-Schwaab et al., 2005; OECD, 2016; Tice et al., 2000). These are indicative of DNA damage produced by either direct or indirect mechanisms. Both techniques are widely used for the evaluation of chemical-induced DNA damage (Himmelstein et al., 2009) and also makes it possible to elucidate the mode of action of chemical carcinogens. Additionally, fetal avian livers express majority of the phase-I and phase-II biotransformation enzymes which can detect chemicals inducing DNA damage post metabolic transformation (Kobets et al., 2018b; Perrone et al., 2004; Rifkind et al., 1979) and they can also efficiently mimic detoxification of chemicals similar to rodent models. Genotoxicity can be induced by direct DNA activity of the parent chemical and/or its metabolite. As such, metabolism plays a crucial role in the bioactivation of many chemicals. This process is often required for the formation of reactive electrophilic intermediates that can then directly react with DNA (Kobets et al., 2019). Bioactivation of different classes of chemicals may differ and produced metabolites may interact with different sites on macromolecules including DNA. Since many *in vitro* systems lack an intrinsic ability to metabolize chemicals, the induced rat liver S9 fraction is used as an exogenous metabolic activation system (Ames et al, 1973; Paolini et al, 1997). However, this exogenous source of metabolic enzymes does not include those that are important for phase II detoxification. Hence, current *in vitro* testing systems generate high number of misleading outcomes in testing and prediction of carcinogens (Kirkland et al., 2007). For analysis of the chicken egg liver response to a xenobiotic, a polycyclic aromatic hydrocarbon, benzo[a]pyrene (B(a)P) was chosen. Many of the chemicals that belong to this group are genotoxic carcinogens (Urwin et al., 2024). Carcinogenic activity of B(a)P involves activation of the Aryl hydrocarbon receptor (AhR), which in turn binds to AhR nuclear translocator and induces the expression of genes involved in B(a)P bioactivation and detoxification. These genes are the cytochrome P450 (CYP) genes CYP1A1, CYP1A2, CYP1B1, as well as glutathione transferase (GST) and Uridine diphosphate (UDP)-glucuronosyltransferase (UGT-1). In order to exhibit genotoxicity, B(a)P requires oxidation by phase I CYP1A1 into B(a)P-7,8-epoxide, which through hydration by microsomal epoxide hydrolase is metabolized to B(a)P-7,8-dihydrodiol (BPD) (Figure 1). BPD is then metabolized to B(a)P-7,8-dihydrodiol-9,10-epoxide (BPDE) by second CYP reaction (Kim et al., 2005). BPDE contains an epoxide ring which is highly reactive with DNA in a time dependent manner. *In vitro* , B(a)P consistently produced negative outcomes in mutagenicity and clastogenicity studies in the absence of metabolic activation, only demonstrating positive outcomes in the presence of exogenous S9 fraction (EPA, 2017).

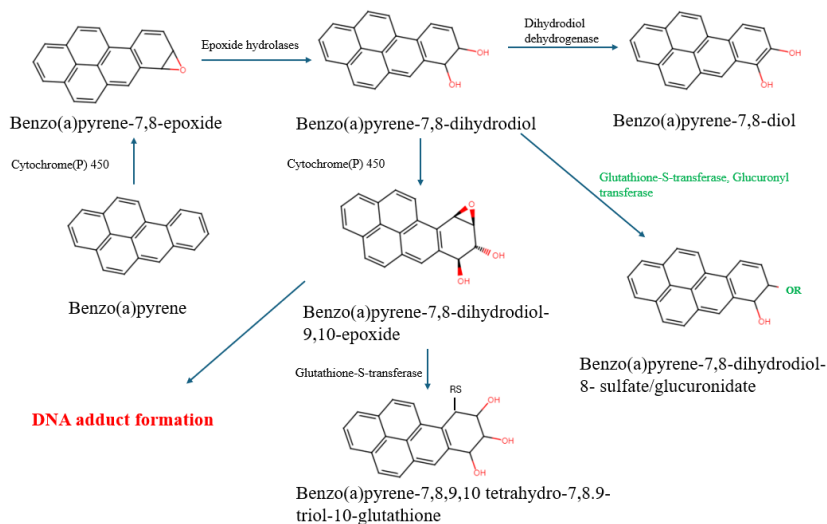


Figure 1: **Metabolism of Benzo (a) pyrene**

To establish the validity of a test system, it is critical to demonstrate target tissue exposure. This is especially true in cases where there is an adverse outcome in the *in vitro* mammalian cell bases assay (ICH S2(R1), 2012). This evidence of target tissue exposure can be demonstrated either by showing cytotoxicity to the target tissue or by directly measuring a drug or related toxic metabolite in the target tissue.

In vivo, assessment of cytotoxicity can be conducted by histopathological evaluation of the target tissue or by analyzing changes in the blood biochemistry values.

The direct measurement of drug-related substances can be performed in blood, plasma, or target tissues. Autoradiographic techniques can be used to assess tissue exposure to these substances. ((ICH S2(R1), 2012; Kirkland et al., 2019). Demonstration of target tissue exposure is critical in validating a NAM that can be used as a follow-up to an *in vitro* assay. Therefore, the goal of this study was to verify that in CEGA tested chemicals can reach the fetal chicken liver (target organ) following administration into the air sac of the fertilized egg at sufficient levels to produce genotoxic effect(s), and to form of sufficient amounts of reactive metabolite(s) from a parent compound upon reaching the target tissue.

MATERIALS and METHODS

A. Chemicals

Solutol HS15 (Kolliphor HS15) (CAS: 70142-34-6), obtained from Sigma-Aldrich (St Louis, MO, USA) prepared as a 20 % aqueous solution (20% HS15) was used as the vehicle. Solutol was used as a vehicle for Benzo(a)pyrene studies. Deionized water was used as a vehicle for acridine orange study. Benzo(a)pyrene (CAS: 50-32-8; [?]96% pure) purchased from Sigma-Aldrich (St Louis, MO, USA) was used in the metabolomics as well as gene expression studies. Acridine orange (CAS: 10127-02-3; pure, [?]55% dye content), purchased from Acros Organics (Bridgewater, NJ, USA), was used for two photon microscopy study.

B. Egg Handling

The protocol of the study is described in detail in Williams et al. (2014) and Thakkar et al. (2024). Briefly, fertilized eggs (SPF Premium) of white leghorn chicken (*Gallus gallus*) were purchased from Charles River

Laboratories (North Franklin, CT). Eggs were weighed, numbered, and randomly divided into control and dosed groups (at least 10 eggs per group). On day 0 incubation day, eggs were placed in automatic egg turners and incubated in GQF Manufacturing Company Hova Bator Model 2362N Styrofoam incubators (Murray McMurray Hatchery, Webster City, IA, USA) at 37 ± 0.5 °C and $60 \pm 5\%$ humidity. Viability was assessed by transillumination on incubation day 8, and eggs that did not develop were discarded. Separate incubators were used for control and dosed eggs to avoid any possible cross contamination. Doses of compounds were selected based on available acute toxicity data (oral LD50 in rodents, extrapolated on ~ 60 g egg). For imaging studies, acridine orange was administered at 10 μ g/egg. For analysis of metabolites and genomic changes, B(a)P was injected at 250 μ g/egg. Test compounds and respective vehicles were administered in total volume of 0.15 ml/egg via 3 daily injections into the air sac on incubation days 9 through 11. For metabolite and gene expression analyses, a group of naïve (non-dosed) eggs that did not receive any injections was also included. The eggs were terminated two to three hours after the last injection. The eggshells were opened, the fetuses removed and decapitated. Fetal weights, including the head, were recorded after removal of the surrounding excess yolk. Viability percentage was calculated based on the ratio of embryo-fetuses alive upon termination to the total number of embryo-fetuses in the group. The abdominal cavity was opened, and the livers were removed, weighed, and processed for further analyses.

C. Two-Photon Microscopy

Instrument Setup: Two-photon imaging of tissue samples was performed using Leica Stellaris 8 DIVE system (Leica Microsystems, Wetzlar, Germany). The microscope is equipped with a mode-locked titanium:sapphire laser for excitation, capable of delivering femtosecond pulses at the desired wavelength. The laser power and wavelength were optimized based on the fluorophores for acridine orange (460/650). The microscope was configured for both two-photon excitation and detection, allowing for deep tissue imaging with high spatial resolution. **Sample Mounting:** Prior to imaging, tissue samples were mounted on to a slide and a drop of water was added with coverslip mounted on top. Care was taken to ensure that the sample was securely positioned and oriented for optimal imaging. **Imaging Parameters:** The imaging parameters, including laser power, wavelength, scanning speed, and image resolution, were carefully optimized. Laser power was adjusted to achieve sufficient signal intensity while minimizing photobleaching and phototoxicity. The scanning speed was optimized to balance imaging speed with signal-to-noise ratio and resolution requirements. Z-stack imaging was performed to capture three-dimensional information about the tissue structure, with the step size adjusted based on the desired axial resolution. **Image Acquisition:** Two-photon imaging was performed using optimized parameters, with image acquisition conducted in both x, y and z dimensions. Z-stack images were acquired by scanning through the tissue volume at consecutive focal planes. Care was taken to minimize exposure to laser light and phototoxic effects on the sample during image acquisition.

D. LC-HRMS

Frozen liver samples were sent to Frontage Laboratories (Exton, PA) for the analysis using LC-HRMS with Xcalibur and Freestyle Compound Discoverer software. **Sample Preparation:** Liver samples were weighed in the non-skirted homogenizing tube containing 0.5 mm Zirconium and mixed with 9-fold of IPA/H₂O=70:30 (weight: volume = 1g: 9 mL) followed by 45 seconds homogenization at 4000 cycles per minute. The homogenized liver samples were volume proportional pooled into three separate mixtures by treatment (untreated, solvent treated, BP treated). 100 μ L of pooled sample were mixed with 200 μ L organic solvent (ACN with 0.1 μ g/mL ISD). Then vortexed and centrifuged for 5min at 13000 rpm. Take 250 μ L of supernatant and dry it down to 100 μ L under N₂ prior to LC/HRMS. **Instrumentation:** The analytical instrumentation utilized in this study consisted of a Thermo Scientific Vanquish Ultra-performance liquid chromatography (UPLC) system equipped with multiple units identified by serial numbers: 8315629, 8315641, 8315545, and 6504418. Coupled to the UPLC system was a Thermo Scientific Q Exactive mass spectrometer identified by the serial number 10374L. **UPLC Conditions:** For chromatographic separation, a mobile phase comprising 0.1% formic acid in water (Mobile Phase A) and 0.1% formic acid in acetonitrile (Mobile Phase B) was

employed. The separation was achieved on a Phenomenex Kinetex BP column (2.6 x 100 mm) using a gradient elution program with varying percentages of Mobile Phase B over time: 5% at 0 min, 5% at 1 min, 75% at 7 min, 95% at 10 min, maintaining 95% until 12 min, returning to 5% at 12.5 min, and equilibrating at 5% until 15 min. The flow rate was set at 0.4 mL/min, and injection volumes ranged from 2 to 10 μ L. **Mass Spec Conditions:** The mass spectrometer was operated in positive ionization mode with a spray voltage of 3.50 kV. Additional parameters included an S-lens RF level of 55, probe heater temperature set at 375°C, and capillary temperature maintained at 325°C. The sheath gas flow rate was set to 45 units, with auxiliary gas at 15 units and sweep gas at 1 unit. Mass spectra were acquired over a range of m/z 150-850 with a full MS resolution of 35,000 and an automatic gain control (AGC) target of 3e6. MS/MS experiments were conducted at a resolution of 17,500, with an AGC target of 1e5, using collision energies (CE) of 30, 40, and 55. **Reagents:** Reagents used in the analysis included Fisher Optima LC/MS grade solvents: water, acetonitrile, methanol, and formic acid. These reagents were chosen to ensure high purity and compatibility with the analytical instrumentation employed in this study.

E. RNA Sequencing

RNA extraction and sequencing from the liver samples were performed at Azenta Life Sciences (South Plainfield, NJ). **RNA extraction:** Total RNA was extracted using Qiagen Rneasy Plus Mini kit following manufacturer's instructions (Qiagen, Hilden, Germany). **Library Preparation with PolyA selection and Illumina Sequencing:** Quantification RNA samples was done using Qubit 2.0 Fluorometer (Life Technologies, Carlsbad, CA, USA) and RNA integrity assessment was done using Agilent TapeStation 4200 (Agilent Technologies, Palo Alto, CA, USA). Prior to library preparation, ERCC RNA Spike-In Mix (Cat: 4456740) from ThermoFisher Scientific, was added to normalized total RNA following manufacturer's protocol. NEB-Next Ultra II RNA Library Prep Kit was used to prepare RNA sequencing libraries (NEB, Ipswich, MA, USA). Enrichment of mRNAs with Oligod(T) beads for a brief time. In the next step at 94 °C enriched mRNAs were fragmented for 15 minutes. Both first and second strand cDNA were synthesized. The cDNA fragments were then end-repaired and adenylated at the 3' ends. Universal adapters were ligated to the cDNA fragments, followed by the addition of indexes and library enrichment through PCR with a limited number of cycles. The validation of the sequencing library was done on Agilent TapeStation (Agilent Technologies, Palo Alto, CA, USA), and quantification was done by using Qubit 2.0 Fluorometer (Invitrogen, Carlsbad, CA) along with quantitative PCR (KAPA Biosystems, Wilmington, MA, USA). On a flowcell the sequencing libraries were clustered. The flowcell was loaded on the Illumina NovaSeq instrument post clustering. Using a 2x150bp Paired End (PE) configuration, the samples were sequenced as a next step. Control software was used to do image analysis and base calling. Raw sequence data (bcl files) generated by the sequencer were converted into fastq files and de-multiplexed using Illumina's bcl2fastq 2.17 software. One mismatch was allowed for index sequence identification. **Data Analysis:** After investigating the quality of the raw data, Trimmomatic v.0.36 was used to trim sequence reads remove possible adapter sequences and poor-quality nucleotides. The trimmed reads were aligned to the human reference genome available on ENSEMBL using the STAR aligner v.2.5.2b, resulting in the generation of BAM files. Unique gene hit counts were calculated using featureCounts from the Subread package v.1.5.2, counting only unique reads that fell within exon regions. The gene hit counts table was then used for downstream differential expression analysis. DESeq2 was employed to compare gene expression between the sample groups, using the Wald test to generate p-values and log2 fold changes. Genes with adjusted p-values < 0.05 and absolute log2 fold changes > 1 were identified as differentially expressed for each comparison. Gene ontology analysis was performed on the statistically significant genes using the GeneSCF software, clustering the genes based on their biological processes and determining their statistical significance using the human GO list. The gene code was converted to gene symbol using Biotools.fr (https://www.biotools.fr/mouse/ensembl_symbol_converter). STRING v. 12.0 and Cytoscape v. 3.1 databases were used for gene mapping, functional enrichment analysis, and network visualization.

RESULTS

A. Target tissue exposure

The results from multiphoton imaging are represented in Figure 2. The visual analysis of the fluorescence intensity indicated that liver tissue in the group that received injections with a fluorescent dye, acridine orange demonstrated an increase in fluorescent staining compared to control group which received injections with deionized water only (Figure 2). This confirms sufficient liver uptake of acridine orange which has reached the target tissue following its administration into the air sac.

Figure 2: **Whole liver imaging using two-photon excitation microscopy.** Images were taken at 500/526 excitation e

B. B(a)P metabolism in CEGA

The viability in the group dosed with B(a)P at a total dose of 250 $\mu\text{g}/\text{egg}$ was 100%. The viability in the vehicle control group was 100%.

The results of metabolism study following B(a)P exposure are shown in Figure 3. No relevant peaks were observed in either naïve (Figure 3A) or solvent control (Figure 3B) groups, indicating that no metabolites were formed in these groups. In contrast, in the livers of chicken embryo-fetuses that received injections with B(a)P, several peaks represent metabolites with transformations on B(a)P ring which were formed at sufficient levels (Figure 3C). The quantification of each transformation and type of transformation is listed in Table 1. These transformations when compared to the established metabolism of B(a)P in other species (Figure 4). Based on the suggested metabolite structures there seems to be similarity in the metabolites and amounts formed between chicken and rodent livers.

Figure 3: **Analysis of metabolites formed over the time in the embryo-fetal chicken liver from the untreated**

Table 1: **Quantification of metabolites detected in the chicken embryo-fetal livers following administration of benzo[a]pyrene (B(a)P).**

Identifier	RT	Observed	Accuracy	Biotransformation of B(a)P	% MS
(min)					
(m/z)					
(ppm)					
M300	3.63	301.0851	-2.7	+3O	2.1
M609a	4.28	610.1852	-0.3	+3O+GSH+2H	14.7
M284a	4.41	285.0910	0.0	+2O	6.5
M609b	4.44	610.1852	-0.3	+3O+GSH+2H	6.0
M284b	4.93	285.0910	0.0	+2O	5.2
M378	5.32	379.0272	0.3	+3O-2H+SO3	7.2
M298	6.00	299.0701	-2.3	+3O-2H	20.1
M268	6.02	269.0956	-1.9	+O	2.0
M443	6.11	444.0899	-0.2	+2O-2H+Mercapturic acid	12.4
M282	7.12	283.0755	-1.4	+2O-2H	23.7

Note: % was calculated by MS response; Gluc, glucuronide; GSH, glutathione; RT, retention time

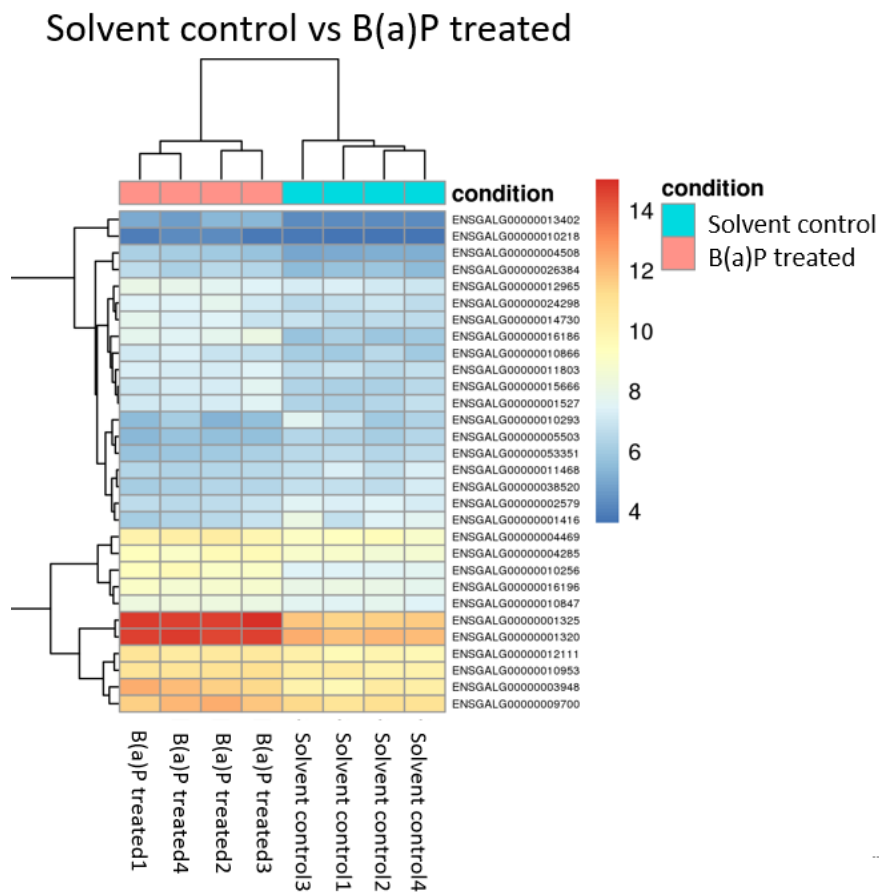


Figure 5: Heatmap showing top 30 significant differentially expressed genes.

Table 2: List of the most abundantly up- and down-regulated genes by benzo(a)pyrene (B(a)P) in the livers of chicken embryo-fetuses

Gene ID	Gene Symbol	Acronym	Function
ENSGALG00000013402	ArhRR	aryl-hydrocarbon receptor repressor	CYP1A1 activity
ENSGALG0000001325	CYP1A1		CYP1A1 activity
ENSGALG00000016186	PDE9A		cGMP activity
ENSGALG0000001320	CYP1A2		CYP1A2 activity
ENSGALG00000010256	TIPARP	TCDD inducible poly (ADP-ribose) polymerase	CYP1A1 activity
ENSGALG0000004508	EYA2	EYA transcriptional coactivator and phosphatase 2	H2Ax; DNA repair activa
ENSGALG0000003948	ALAS1	5'-aminolevulinatase synthase 1	catalyzes the rate-limiting
ENSGALG00000026384	PCSK4	proprotein convertase subtilisin/kexin type 4	subtilisin-like proprotein
ENSGALG0000001416	ADRA1B	adrenoceptor alpha 1B	Alpha-1-adrenergic recept
ENSGALG00000010293	RBP	Riboflavin transport	

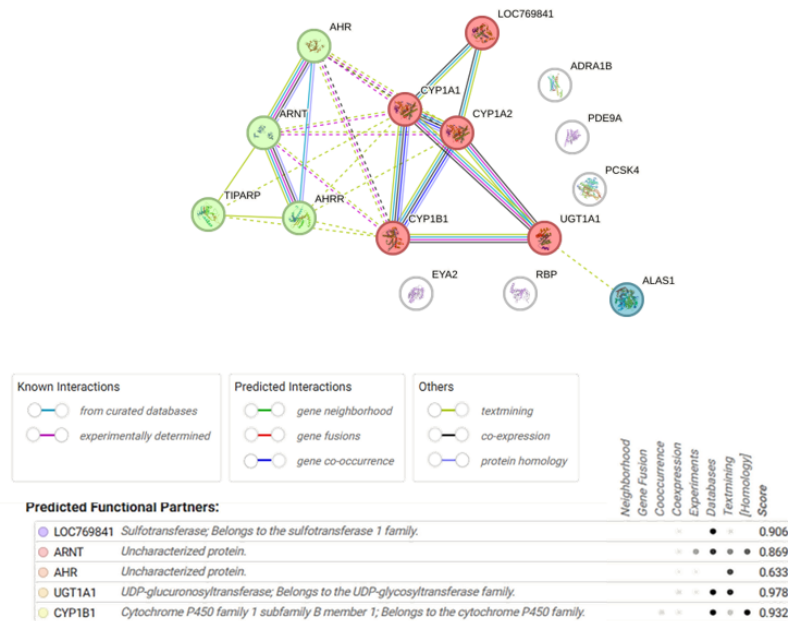


Figure 7: Protein-protein interactions among the identified significantly expressed genes. Figure was created using

Table 3: Functional enrichments of queried significantly deregulated genes

Term ID	Term description
Biological Process	
GO:0006805	Xenobiotic metabolic process
Molecular Function	
GO:0070330	Aromatase activity
Cellular Component	
GO:0034751	Aryl hydrocarbon receptor complex
Local Network Cluster (STRING)	
CL:3288	Steroid hormone biosynthesis
CL:24010	Mixed, incl. Ubiquitin family, and WWE domain, subgroup
CL:3291	Atorvastatin ADME, and Cytochrome P450, E-class, group I, CYP1
CL:3302	Mixed, incl. Response to mycotoxin, and Cytochrome P450, E-class, group I, CYP2D-1
CL:19140	Motif C-terminal to PAS motifs (likely to contribute to PAS structural domain), and P
KEGG Pathways	
gga00140	Steroid hormone biosynthesis
gga00980	Metabolism of xenobiotics by cytochrome P450
gga00380	Tryptophan metabolism
gga00830	Retinol metabolism
gga00860	Porphyryn and chlorophyll metabolism
Reactome Pathways	
GGA-211859	Biological oxidations
GGA-211976	Endogenous sterols
GGA-8937144	Aryl hydrocarbon receptor signalling
GGA-211981	Xenobiotics

Term ID	Term description
GGA-9753281	Paracetamol ADME
Subcellular Localization	
GOCC:0034751	Aryl hydrocarbon receptor complex
Protein Domain and Features	
PF00067	Cytochrome P450
IPR008066	Cytochrome P450, E-class, group I, CYP1
SM00091	PAS domain
SM00353	Helix loop helix domain

A. Figure 8: Network visualization for selected enriched pathways. A. WikiPathway WP2873 - Aryl hydrocarbon
 B.

DISCUSSION

To evaluate the CEGA model as an *in vivo* NAM, it is critical to assess target tissue exposure. Since the injections in CEGA are done in the air space of fertilized eggs, there is a layer of eggshell membrane which xenobiotics must cross in order to reach the target tissue, which is liver. To demonstrate target tissue exposure and sufficient metabolism after reaching target tissue multiphoton microscopy, metabolite analysis, and genomic studies were conducted. For multiphoton microscopy, acridine orange was selected as an appropriate fluorescence dye since the molecular weight of acridine orange is in the range of B(a)P. The results indicated that even though the chemical was injected into the airspace, it penetrated the eggshell membrane and reached the liver (Figure 2), resulting in sufficient liver uptake. To study metabolism in CEGA, B(a)P was used as a chemical of choice, since it is known to produce its genotoxic effect post metabolic activation. Moreover, previous studies in CEGA confirmed that B(a)P forms DNA adducts and DNA strand breaks in the livers of chicken embryo-fetuses (Williams et al., 2014). B(a)P-7,8 dihydrodiol-9,10-epoxide is the reactive metabolite known to covalently bind to DNA forming adducts and producing adverse effects (Figure 1). Additionally, metabolism of B(a)P has been well documented in animal studies, which allows for comparison between the metabolites formed in the livers of chicken embryo-fetuses and other species. The characterization of metabolites formed in CEGA following exposure to B(a)P confirmed that the majority of these six metabolites were also observed in the rat (Figure 4), Two additional metabolites were formed in the chicken livers. These were identified as M378 and M300, and formed at 7.2 and 2.1%, respectively. M378 metabolite had an additional of three oxygen molecules (3O), removal of two hydrogen groups (-2H) and addition of one sulfate group (SO₃), whereas M300 metabolite had additional three oxygen (3O) on B(a)P ring. However, M378 formation is also justified and follows similar pathway as mentioned in IARC document (IARC 1983) which states that B(a)P is metabolized initially by the microsomal CYP systems to several arene oxides. Once formed, these arene oxides may rearrange spontaneously to phenols, undergo hydration to the corresponding trans-dihydrodiols in a reaction catalyzed by microsomal epoxide hydrolase, or react covalently with GSH, either spontaneously or in a reaction catalyzed by cytosolic GST (IARC 1983). Overall, the findings in the metabolism study confirmed that B(a)P metabolism in CEGA aligns with the established metabolic pathway in rodents (Decker et al. 2009). Another similarity was observed with the animal study of orally administered B(a)P in F344 rats, which found a half-life of B(a)P in rat liver to be 12 hours, suggesting that unmodified/unmetabolized B(a)P will be 100% converted to its metabolites 24 hours post-exposure (Ramesh et al., 2001). In CEGA, 100% of administered B(a)P was converted to its relevant metabolites. The toxic precursor, (B(a)P-7,8-dihydrodiol), was formed at 23.1% 48-hour post treatment in embryo-fetal chicken livers. In rat liver, however, B(a)P-7,8-dihydrodiol was only present at 10% 48-hour post administration with its peak liver concentration at ~30% 24-hour post treatment after single dose of

100 mg/kg bw of B(a)P (Ramesh et al., 2001). Formation of the reactive metabolite, B(a)P-7,8 dihydrodiol-9,10-epoxide, which in CEGA was formed at 20%, is likely to be responsible for formation of DNA adducts observed in the embryo-fetal chicken livers (Williams et al., 2014). The difference in the amount of metabolite formed in CEGA and rodent study mentioned above may also be due to single oral administration in Ramesh et al., 2001 study as compared to three different dose in CEGA studies. The analyses of the differential gene expression in the embryo-fetal chicken livers following exposure to B(a)P also confirmed that the compound upregulated the expression of genes responsible for its bioactivation (Tables 2 and 3, Figure 7). Specifically, out of 10 significantly deregulated genes with $>\log$ 2-fold changes, three were involved in the activity of CYP1A1 and CYP1A2 isoenzymes. Other identified genes were also involved in the activity of DNA strands break mediated gene H2AX and DNA repair mediated gene RNA polymerase II. These results support the conclusion that B(a)P at a total dose of 250 ug/ egg upregulates expressions of CYP1A genes which affects the activity of CYP1A1 (Suppl. Figure 1), leading to formation of reactive metabolite, BPDE, resulting in DNA damage, and activating DNA repair mechanisms. In addition to the upregulation of genes involved in CYP1A1 activity, an increase was also observed in the expression of genes which regulate CYP1A1 by negative feedback loop. Specifically, upregulation of AhR repressor and TCDD Inducible Poly (ADP-Ribose) Polymerase (TiPARP) genes (Table 2) can negatively regulate CYP1A1 activity. This also add to the fact that with B(a)P treatment there was significant increase in CYP1A1 activity, which is a critical enzyme for metabolizing B(a)P leading to toxic metabolite, but gene regulating CYP1A1 expression by negative feedback mechanism were also present in chicken livers. Similarities between the expressions of CYP1A1 and CYP1A2 genes in the embryofetal chicken livers following dosing with B(a)P were observed with the published data in rodents and human cells. For example, expressions of CYP1A1 and CYP1A2 genes in the livers of Wistar rats that received B(a)P at a single dose of 150 mg/kg bw by oral gavage was significantly increased by 2990 and 27.7 folds, respectively (Dračinská et al., 2021). In the study with human hepatocellular carcinoma cell line (HepG2) which was incubated with 2 μ M of B(a)P, CYP1A1 showed a 93-fold and 79-fold increase in expression on microarray 12- and 24-hours post-dosing, respectively, whereas RNA-seq demonstrated a 199-fold (at 12 hours) and 214-fold (at 24 hours) increases in CYP1A1 expression (Van Delft et al.; 2012). In the human tissue organoid cultures, differentiated liver had significantly higher (24-fold) CYP1A1 levels compared to undifferentiated samples, at basal level. After exposure to 50 μ M of B(a)P, induction of CYP1A1 in differentiated liver organoids was around double compared to that in undifferentiated organoids (~4500- and 2000-fold, respectively), relative to control. At 12.5 μ M, a 287-fold change compared to undifferentiated control was observed only in differentiated organoids. Induction of CYP1A1 was also significant at both concentrations of B(a)P compared to differentiated control (Caipa Garcia et al., 2023). These results are consistent with findings in CEGA which demonstrated a fold change of 1024 folds for CYP1A1 activity combined (ENSGALG00000013402 and ENSGALG0000001325) and 16 folds for CYP1A2 activity (Table 2).

CONCLUSION

The findings in the current study in CEGA demonstrate sufficient liver uptake, metabolism and gene expression modulations which resemble that of rodents, which confirm the utility of the model as a NAM for assessment of genotoxic potential of chemicals.

REFERENCES

Animals (Scientific Procedures) Act 1986 Amendment Regulations. (2012). Ates, G., Doktorova, T. Y., Pauwels, M., & Rogiers, V. (2014). Retrospective analysis of the mutagenicity/genotoxicity data of the cosmetic ingredients present on the Annexes of the Cosmetic EU legislation (2000–12). *Mutagenesis*, 29(2), 115-121. Caipa Garcia, A. L., Kucab, J. E., Al-Serori, H., Beck, R. S. S., Fischer, F., Hufnagel, M., Hartwig, A., Floeder, A., Balbo, S., Francies, H., Garnett, M., Huch, M., Drost, J., Zilbauer, M., Arlt, V. M., &

Phillips, D. H. (2023). Metabolic activation of benzo[a]pyrene by human tissue organoid cultures. *International Journal of Molecular Sciences*, *24*(1), 606. <https://doi.org/10.3390/ijms24010606>

Decker, M., Arand, M., & Cronin, A. (2009). Mammalian epoxide hydrolases in xenobiotic metabolism and signalling. *Archives of Toxicology*, *83*(4), 297-318. <https://doi.org/10.1007/s00204-009-0416-0>

Dračínská, H., Indra, R., Jelínková, S., Černá, V., Arlt, V. M., & Stiborová, M. (2021). Benzo[a]pyrene-induced genotoxicity in rats is affected by co-exposure to Sudan I by altering the expression of biotransformation enzymes. *International Journal of Molecular Sciences*, *22*(15), 8062. <https://doi.org/10.3390/ijms22158062>

Duan, J. D., & Williams, G. M. (2016). *In vitro* photochemical induction of kojic acid-DNA adducts. *Toxicol Open Access*, *2*(115). <https://doi.org/10.4172/2476-2067.1000115>

frEnsembl gene database. (n.d.). *Gallus gallus*. Retrieved from https://mart.ensembl.org/Gallus_gallus/Info/Index

Environmental Protection Agency (EPA). (2017). *Toxicological review of benzo[a]pyrene*. Retrieved from <https://iris.epa.gov/static/pdfs/0136tr.pdf>

European Parliament and Council. (2003). Directive 2003/15/EC of the European Parliament and of the Council of 27 February 2003 amending Council Directive 76/768/EEC on the approximation of the laws of the Member States relating to cosmetic products. *Official Journal of the European Union*, *66*, 26-35.

Food and Drug Administration (FDA). (2020). *Safety testing of drug metabolites: Guidance for industry (Revision 2)*. Himmelstein, M. W., Boogaard, P. J., Cadet, J., Farmer, P. B., Kim, J. H., Martin, E. A., Persaud, R., & Shuker, D. E. (2009). Creating context for the use of DNA adduct data in cancer risk assessment: II. Overview of methods of identification and quantitation of DNA damage. *Critical Reviews in Toxicology*, *39*, 679-694.

Hughes, A. F. W. (1953). The growth of embryonic neurites. A study of cultures of chick neural tissues. *Journal of Anatomy*, *87*, 150-162.

IARC. (1983). Polynuclear aromatic compounds, Part 1, chemical, environmental, and experimental data. *IARC Monographs on the Evaluation of Carcinogenic Risks to Humans*, *32*, 1-453.

Iatropoulos, M. J., Kobets, T., Duan, J. D., Brunnemann, K. D., Vock, E., Deschl, U., & Williams, G. M. (2017). Chicken egg fetal liver DNA and histopathologic effects of structurally diverse carcinogens and non-carcinogens. *Experimental Toxicology and Pathology*. ICH S2(R1). (2011). *Guidance on genotoxicity testing and data interpretation for pharmaceuticals intended for human use*. ICH Harmonised Tripartite Guideline.

Kim, H.-B., Um, J.-Y., Chung, B.-Y., Kim, J.-C., Kang, S.-Y., Park, C.-W., & Kim, H.-O. (2022). Aryl hydrocarbon receptors: Evidence of therapeutic targets in chronic inflammatory skin diseases. *Biomedicines*, *10*(5), 1087. <https://doi.org/10.3390/biomedicines10051087>

Kirkland, D., Aardema, M., Banduhn, N., Carmichael, P., Fautz, R., Meunier, J., & Pfuhler, S. (2007). *In vitro* approaches to develop weight of evidence (WoE) and mode of action (MoA) discussions with positive *in vitro* genotoxicity results. *Mutagenesis*, *22*(3), 161-175.

Kirkland, D., Uno, Y., Luijten, M., Beevers, C., van Benthem, J., Burlinson, B., Dertinger, S., Douglas, G. R., Hamada, S., Horibata, K., Lovell, D. P., Manjanatha, M., Martus, H. J., Mei, N., Morita, T., Ohyama, W., & Williams, A. (2019). *In vivo* genotoxicity testing strategies: Report from the 7th International Workshop on Genotoxicity Testing (IWGT). *Mutation Research/Genetic Toxicology and Environmental Mutagenesis*, *847*, 403035. <https://doi.org/10.1016/j.mrgentox.2019.03.008>

Kobets, T., Duan, J. D., Brunnemann, K. D., Etter, S., Smith, B., & Williams, G. M. (2016). Structure-activity relationships for DNA damage by alkenylbenzenes in turkey egg fetal liver. *Toxicological Sciences*, *150*, 301-311.

Kobets, T., Duan, J. D., Brunnemann, K. D., Iatropoulos, M. J., Etter, S., Hickey, C., Smith, B., & Williams, G. M. (2018a). In ovo testing of flavor and fragrance materials in Turkey Egg Genotoxicity Assay (TEGA), comparison of results to *in vitro* and *in vivo* data. *Food and Chemical Toxicology*, *115*, 228-243.

Kobets, T., Iatropoulos, M. J., Duan, J. D., Brunnemann, K. D., Iacobas, D. A., Iacobas, S., Vock, E., Deschl, U., & Williams, G. M. (2018b). Expression of genes encoding for xenobiotic metabolism after exposure to dialkylnitrosamines in the chicken egg genotoxicity alternative model. *Toxicological Sciences*, *166*, 82-96.

Kobets, T., Iatropoulos, M. J., & Williams, G. M. (2019). Mechanisms of DNA-reactive and epigenetic chemical carcinogens: Applications to carcinogenicity testing and risk assessment. *Toxicology Research (Cambridge)*, *8*(2), 123-145. <https://doi.org/10.1039/c8tx00250a>

Matthews, J. (2017). AHR toxicity and signaling: Role of TIPARP and ADP-ribosylation. *Current Opinion in Toxicology*, *2*, 50-57. <https://doi.org/10.1016/j.cotox.2017.01.013>

National Library of Medicine (NLM). (n.d.). *Gene*. Retrieved from <https://www.ncbi.nlm.nih.gov/gene/396052>

Organization for Economic Co-operation and Development (OECD). (2016). *OECD Guidelines for the Testing of Chemicals Section 4, Test No. 489. In Vivo Mammalian Alkaline Comet Assay*. OECD Publishing, Paris.

Perrone, C. E., Ahr, H. J., Duan, J. D., Jeffrey, A. M., Schmidt, U., Williams, G. M., & Enzmann, H.

G. (2004). Embryonic turkey liver: Activities of biotransformation enzymes and activation of DNA-reactive carcinogens. *Archives of Toxicology*, *78*, 589-598. Phillips, D. H., & Arlt, V. M. (2014). 32P-postlabeling analysis of DNA adducts. *Methods in Molecular Biology*, *1105*, 127-138. Ramesh, A., Inyang, F., Hood, D. B., Archibong, A. E., Knuckles, M. E., & Nyanda, A. M. (2001). Metabolism, bioavailability, and toxicokinetics of benzo(alpha)pyrene in F-344 rats following oral administration. *Experimental Toxicology and Pathology*, *53*(4), 275-290. <https://doi.org/10.1078/0940-2993-00192> Randerath, K., Reddy, M. V., & Gupta, R. C. (1981). 32P-labeling test for DNA damage. *Proceedings of the National Academy of Sciences*, *78*, 6126-6129. Reddy, M. V., & Randerath, K. (1986). Nuclease P1-mediated enhancement of sensitivity of 32P-postlabeling test for structurally diverse DNA adducts. *Carcinogenesis*, *7*, 1543-1551. Ren, N., Atyah, M., Chen, W. Y., et al. (2017). The various aspects of genetic and epigenetic toxicology: Testing methods and clinical applications. *Journal of Translational Medicine*, *15*, 110. <https://doi.org/10.1186/s12967-017-1218-4> Thakkar, Y., Kobets, T., Api, A. M., Duan, J. D., & Williams, G. M. (2024). Assessment of genotoxic potential of fragrance materials in the chicken egg assays. *Environmental and Molecular Mutagenesis*, *65*(8), 261-274. <https://doi.org/10.1002/em.22627> Tice, R. R., Agurell, E., Anderson, D., Burlinson, B., Hartmann, A., Kobayashi, H., Miyamae, Y., Rojas, E., Ryu, J. C., & Sasaki, Y. F. (2000). Single cell gel/comet assay: Guidelines for *in vitro* and *in vivo* genetic toxicology testing. *Environmental and Molecular Mutagenesis*, *35*, 206-221. D.J. Urwin, E. Tran, A.N. Alexandrova, Relative genotoxicity of polycyclic aromatic hydrocarbons inferred from free energy perturbation approaches, *Proc. Natl. Acad. Sci. U.S.A.* *121* (37) e2322155121, <https://doi.org/10.1073/pnas.2322155121> (2024). Van Delft, J. H. M., Mathijs, K., Staal, Y. C. M., et al. (2010). Time series analysis of benzo[a]pyrene-induced transcriptome changes suggests that a network of transcription factors regulates the effects on functional gene sets. *Toxicological Sciences*, *117*, 381-392. <https://doi.org/10.1093/toxsci/kfq214> Williams, G. M., Duan, J. D., Brunnemann, K. D., Iatropoulos, M. J., Vock, E., & Deschl, U. (2014). Chicken fetal liver DNA damage and adduct formation by activation-dependent DNA-reactive carcinogens and related compounds of several structural classes. *Toxicological Sciences*, *141*(1), 18-28. Ye, G., Lu, W., Zhang, L., Gao, H., Liao, X., Zhang, X., Zhang, H., Chen, J., & Huang, Q. (2022). Integrated metabolomic and transcriptomic analysis identifies benzo[a]pyrene-induced characteristic metabolic reprogramming during accumulation of lipids and reactive oxygen species in macrophages. *Science of The Total Environment*, *829*, 154685. <https://doi.org/10.1016/j.scitotenv.2022.154685>

SUPPLEMENTARY MATERIALS

Suppl. Fig. 1. Activity of CYP1A1 enzyme in the embryo-fetal chicken livers following exposure to benzo(a)
